SDEMPED 2005 - International Symposium on
Diagnostics for Electric Machines, Power Electronics and Drives
Vienna, Austria, 7-9 September 2005

Detection of incipient rotor cage fault and mechanical abnormalities in induction motor using global modulation index on the line current spectrum

G. Didier[1], E. Ternisien[2] and H. Razik[1], *Senior Member, IEEE*
[1]Groupe de Recherches en Electrotechnique et Electronique de Nancy
GREEN - UHP - UMR - 7037
[2]Centre de Recherche en Automatique de Nancy
CRAN - UHP - UMR - 7039
Université Henri Poincaré - Nancy 1 - BP 239
F – 54506 Vandœuvre-lès-Nancy, Cedex, France
Tel : +33 3 83 68 41 42 Fax : +33 3 83 68 41 33
e-mail : Gaetan.Didier@green.uhp-nancy.fr

***Abstract*— Asynchronous motors is nowadays the most used in industrial process. In this paper we describe a new approach to detect incipient broken rotor bar and mechanical abnormalities. We use the magnitude of components created in the line current and the instantaneous power spectra of one stator phase to detect the presence of these faults in induction motors. We show that the study of components created by space harmonics in the stator current allows us to differentiate a broken rotor bar to a load torque variation. First, we have looked the effects of these faults with a simulation model. Tanks to this study, fault components we have to supervise are localized in power spectra. Secondly, a load torque oscillation and several rotor cage faults were studied with various load level. Experimental results prove the efficiency of the proposed method.**

***Index Terms*— Induction motor, Diagnosis, Modulation indexes, Incipient broken rotor bar, Load torque oscillation.**

I. Introduction

In this paper, we proposed a method based on space harmonics study to differentiate a broken rotor bar to a load torque variation. The broken rotor bar and load torque oscillation can be connected to the analysis of the global modulation index [5]. We estimate the global modulation index corresponding to the contribution of all faults components present in line current spectrum. In order to find the frequency and the amplitude of each component, we use the power spectral density of the instantaneous power of one stator phase [7] [8]. We show that using of this signal improves the detection of components created by the two types of defects [9]. First, we study the effects of the two faults on the line current with a induction motor model. This analysis permit to define which are the most significant components to diagnose the defect. Thereafter, we carry out experimental tests to validate the suggested method. The study show that thanks to the components created by space harmonics, we can differentiate a rotor fault to a mechanical fault.

II. Induction motor model

Space harmonics are the result of the distribution of the coil in the stator slots. They directly modify the magnetomotive force (MMF) of the induction machine. We have introduced these harmonics in a simulation model by modifying the leakage inductances of stator circuits and mutual inductances between stator and rotor circuits. The different calculus for the evaluation of these inductances and the description of the simulation model are explained in [4].

The study of a broken rotor bar and a load torque variation effects on the induction motor model permits to identify components that we must supervise to detect these type of faults in the power spectrum of the line current. First, we create a rotor fault by introducing a broken rotor bar in the simulation model. This broken bar induces a modification of the rotor induction (fundamental and space harmonics) what result in an increase of components harmonics amplitude in the line current spectrum. The power spectrum of the line current in this case is show on figure 1(a) in the frequency band [0 - 100] Hz. As we can see, components appear at frequencies $(1 \pm 2ks)f_s$ around the fundamental component f_s [1]. If we study the frequency band [100 - 1000] Hz of this spectrum (figure 1(b)), additional components appear at frequencies given by the relation [3] :

$$f_{sh_k} = (x(1-s) \pm (1+2\eta)s)\, f_s \tag{1}$$

where $x = k/p$ represents the space harmonic order (3, 5, 7, 9, ...), s the slip of the induction motor and η can take values 0, 1, 2, 3, ... In this paper, these components will be named C_{sh_x}.

In the case of a load torque oscillation (we chose a frequency oscillation equal to $2sf_s$), we can see on figure 2(a) that components appear at the same frequencies that broken rotor bar, i.e. $(1 \pm 2ks)f_s$. Consequently, if we study only these components to diagnose the induction motor, we will not know if we have a rotor fault or a mechanical abnormality. In this case, the study of space harmonics is essential. Indeed, as we can show on figure 2(b), the load torque oscillation does not disturb the components created by these harmonics. We have not any additional components in this frequency band because the induction rotor is not modified. Consequently, the monitoring of space harmonics components allows to

differentiate a broken rotor bar to a load torque oscillation at $2sf_s$.

To determine the frequency of these components, the value of the slip of the induction motor is required. For that, the relative power spectral density of the instantaneous power of one stator phase is used. Indeed, we find in this spectrum the fault components created by a rotor fault or a load torque oscillation in a frequency band [0 - 100] Hz well-bounded [6] [7].

III. Calculation of the slip of the induction motor

Appearance of broken rotor bar or load torque oscillation at $2sf_s$ induces, in the stator current, additional frequencies at $(1 \pm 2ks)f_s$. These fault created an amplitude modulation and a phase modulation in the line current. If we look at figures 1(a) and 2(a), we can see that we do not have the same amplitude for the component at $(1-2s)f_s$ and the component at $(1 + 2s)f_s$ [2]. This difference is caused by the inertia of the induction motor and by the weak modulation phase presents in the line current. Consequently, we do not have an amplitude modulation with a perfectly symmetrical modulation law compared to the carrier frequency : the sidebands magnitude on the left and on the right are different. Moreover, the number of components at the left can be different that the number of components at the right. Consequently, the line current expression can be written :

$$i_s(t) = i_{s0}(t) + \sum_{k=1}^{K_l} \frac{\sqrt{2}I_s m_{c_k}}{2} \cos((\omega_s - k\omega_f)t - \varphi) + \sum_{k=1}^{K_r} \frac{\sqrt{2}I_s m'_{c_k}}{2} \cos((\omega_s + k\omega_f)t - \varphi) \quad (2)$$

In this expression, m_{c_k} and m'_{c_k} represent the modulation index of the left component k and the modulation index of the right component k. Terms K_l and K_r represent respectively the number of components at the left and at the right of the carrier frequency f_s presents in the line current spectrum when a fault appears. The expression of the instantaneous power of one phase gives :

$$\begin{aligned} p_s(t) &= p_{s0}(t) + \sum_k \frac{m_{p_k} V_s I_s}{2} \cos((2\omega_s - k\omega_f)t - \varphi) \\ &+ \sum_k \frac{m'_{p_k} V_s I_s}{2} \cos((2\omega_s + k\omega_f)t - \varphi) + \\ &+ \sum_k \frac{V_s I_s}{2} [m_{p_k} + m'_{p_k}] \cos\varphi \cos(k\omega_f t) \\ &+ \sum_k \frac{V_s I_s}{2} [m'_{p_k} - m_{p_k}] \sin\varphi \sin(k\omega_f t) \end{aligned} \quad (3)$$

We have, in the instantaneous power spectrum, the presence of a spectral peak at the modulation frequency $f_f = \omega_f/(2\pi)$. The latter, subsequently called a characteristic component, provides an extra piece of diagnostic information about the health of the motor. Its amplitude depends on phase angle φ and on modulation indexes m_{p_1} and m'_{p_1}. In our case, it is this component which is used for the calculation of the slip s. Indeed, with the estimation of the $2sf_s$ frequency, we will know the speed of the rotor and consequently, we could estimate the exact frequencies of the fault components in the line current spectrum. The detection of these components is easier in the instantaneous power spectrum than in the line current spectrum because we find them in a frequency band well-bounded. Indeed, it would be difficult to filter out the fundamental component of the stator current without affecting the sideband component. In opposite, the characteristic component in the spectrum of instantaneous power can easily be separated from the DC component by compensation of the latter. The spectrum of the power provides easier filtering conditions than that of the stator current [9].

IV. Evaluation of line current modulation indexes

According to the amplitude modulation theory, if several sinusoidal signals modulate the same carrier wave, the power of this wave does not change while the modulating signals increase the power contained in the sidebands. Since the modulation index is proportional to the amplitude of the modulating signal, different modulation indexes correspond to different modulating signals. The global modulation index m_{t_c} of the line current is defined so that the power of the sidebands equals the sum of powers of each sideband. Consequently, the expression of the global modulation index m_{t_c}, by integrating the terms K_l and K_r becomes:

$$m_{t_c}^2 = \sum_{k=1}^{K_l} m_{c_k}^2 + \sum_{k=1}^{K_r} m'^2_{c_k} \quad (4)$$

Moreover, for each modulation frequency $(1 \pm 2ks)f_s$, we can deduce its modulation index m_k by dividing its estimated amplitude $A_{s_k} = m_k A_c/2$ by the amplitude of the carrier frequency $A_c = \sqrt{2}I_s$:

$$\frac{A_{s_k}}{A_c} = \frac{m_k A_c}{2} \frac{1}{A_c} = \frac{m_k}{2} \Longrightarrow m_k = \frac{2A_{s_k}}{A_c} \quad (5)$$

The same study can be done with space harmonics components. If we complete expression (2) to integer these space harmonics, we obtain the line current expression given in eq. 6. where the term $(2x + 1)$ represents the number of space harmonics that we want to take into account for the diagnosis of the induction motor. With this last expression and referring to eq. (5) , a global modulation index specific to the space harmonic $(2x + 1)$ can be calculated with the expression:

$$m_{tsh_{(2x+1)}}^2 = \sum_{\eta=0}^{K_l} m_{sh_{(2x+1)_\eta}}^2 + \sum_{\eta=0}^{K_r} m'^2_{sh_{(2x+1)_\eta}} \quad (7)$$

Let us note that in this study, the number of space harmonics considered is equal to 13 ($x = 6$). We can connect the detection of a broken rotor bar to the analysis of these global modulation indexes. In fact, if these indexes increase with index m_{tc}, we will have a broken rotor bar and not a load torque oscillation. In the contrary case, we will have a load torque oscillation and not a broken rotor bar. We have described the method used to monitor the induction motor.

$$
\begin{aligned}
i_s(t) \quad = \quad & i_{s0}(t) + \sum_{k=1}^{K_l} \frac{\sqrt{2} I_s m_{c_k}}{2} \cos((1-2ks)\omega_s t - \varphi) + \sum_{k=1}^{K_r} \frac{\sqrt{2} I_s m'_{c_k}}{2} \cos((1+2ks)\omega_s t - \varphi) \\
& + \sum_{x=1}^{\infty} \sum_{\eta=0}^{K_l} \frac{\sqrt{2} I_s m_{sh_{(2x+1)\eta}}}{2} \cos(((\mathbf{2x+1})(1-s) - (1+2\eta)s)\,\omega_s t - \varphi) \\
& + \sum_{x=1}^{\infty} \sum_{\eta=0}^{K_r} \frac{\sqrt{2} I_s m'_{sh_{(2x+1)\eta}}}{2} \cos(((\mathbf{2x+1})(1-s) + (1+2\eta)s)\,\omega_s t - \varphi)
\end{aligned} \tag{6}
$$

V. Experimental results

The test-bed used in the experimental investigation is a three-phase, 50 Hz, 2-poles, 3 kW induction motor. Several rotors cage type with 28 rotor bars could be interchanged. The Bartlett peridogram with a Hanning's window is computed and the power spectral density of instantaneous power and line current is plotted [10] [11]. The voltage and the line current measurements are taken for the motor operating at the nominal rate. For both variables, the sampling frequency is 2 kHz and each data length is equal to 2^{18} samples. Each spectrum is calculated with 32768 points (length for the average of the Bartlett periodogram). Two levels of rotor faults are studied: a partially broken rotor bar and one broken rotor bar. Two resistor banks serve as a load for the generator. A first bank is used as a fixed load, while the second one can be switched on and off by a power electronic switch in order to introduce mechanical abnormalities (load torque oscillation)[7].

A. Detection of a rotor fault

To make a decision about the state of the induction motor, we define a reference witch is obtain with an healthy motor. Figures 3(a) and 4(a) give us the power spectral density of the line current and instantaneous power of one stator phase in the case of a healthy operation with a constant and nominal load torque. We can observed the presence of a component at frequency $2sf_s$ in the instantaneous power spectrum and components at $(1 \pm 2ks)f_s$ in the line current spectrum. The presence of these components means that we have a modulation amplitude in the stator current witch is the result of a natural asymmetry of the rotor. Indeed, like the cage of the asynchronous motors is not perfect, there exist on any type of induction machines, a backward rotating field in the air gap at frequency $-gf_s$. This is this imperfection which induces, in the line current and instantaneous power, the appearance of these modulations. In the case of our healthy motor, they are these amplitude modulations and the global modulation index associated which will be used as the reference. For each acquisition, the global modulation index is calculated and compared with the reference to evaluate the state of the rotor cage.

As we shown in section III, when a broken rotor bar occurs, this asymmetry increases and several sidebands appear at frequencies $2ksf_s$ in the instantaneous power spectrum and $(1 \pm 2ks)f_s$ in the line current spectrum (figures 3(b) and 4(b)). The first frequency easily detectable is the $2sf_s$ one in the instantaneous power spectrum because it is the component with the highest magnitude in the considered band $B_{lf} = [0.2 - 35]$ Hz. Then, we search all maxima that magnitude are at frequencies $2ksf_s$ with a greater accuracy (the tolerance is below 1%) and above a threshold defined as the mean of the spectrum in the band B_{lf}. This information gives us the value of the slip s and the number of components K_{pn}. The terms K_l and K_r in eq. (6) can be replaced by the value of K_{pn} because we have chosen to detect an equal number of components on the right and on the left of the carrier frequency f_s of the line current spectrum. With the slip s, we calculate the frequencies $(1 \pm 2ks)f_s$ and $(x(1-s) \pm (1+2\eta)s)\,f_s$ of the fault components to evaluate their amplitudes. Then, we estimate the modulation index of each modulation frequency in the same way as the eq. (5). Finally, with eq. (4) and eq. (7), we give global modulation indexes on the line current m_{tc} and $m_{tsh_{(2x+1)}}$.

The value of global modulation indexes m_{tc} and $m_{tsh_{(2x+1)}}$ in the case of a healthy rotor, a partially broken rotor bar and one broken rotor bar at different load level are given in Table I. Table I gives the state of the motor (for example, we note H-L100 the case of a healthy rotor with 100% load, 05b-L75 for a partially broken rotor bar with 75% load and 1b-L25 for a broken rotor bar with 25% load), the value of the $2sf_s$ frequency detected, the speed of the rotor calculated with this frequency, the number of component K_{pn} detected in the frequency band [0.2 - 35] Hz of the instantaneous power spectrum, the value of the global modulation index m_{tc} of the line current and its increasing in comparison with the healthy operation $\mathcal{A}(m_{tc})$. As we can see, the global modulation index m_{tc} increases when a incipient rotor fault occurs in the rotor cage (partially broken rotor bar). In the case of one broken rotor bar, the increasing is very important in comparison with the healthy operation of the induction motor. We note an augmentation even of a load torque equal to 0%. Moreover, we can see that for some cases, the number of components K_{pn} increases too.

If we look at global modulation indexes of space harmonics, we can see that they also increase when a partially or completely broken rotor bar appears. Among all these indexes, we note that indexes of space harmonics 5 and 7 increase the most significantly (figures 5(a) and 5(b)). The others indexes like $m_{tsh_{(3)}}$ or $m_{tsh_{(9)}}$ are not modified because they depend on the winding factor of the induction motor analyzed. In our case, this winding factor is equal to 2/3. This value limit the effect of harmonics $3k$ (k is an integer) in the magnetomotive force of the air gap. It is for this reason that these indexes do not increase when the rotor cage is failing.

The global modulation indexes of the space harmonics

when the load torque level is equal to 0% were not studied because the faults components detected were not the good components. This error is due to the low value of the slip. With the use of a tolerance of 1%, frequencies bands where the space harmonics frequencies are evaluated (eq. 1) are overlaps. Consequently, the choice of the maximum component in the frequencies bands considered is identical for the frequency $(5(1-s)-s)\,f_s$ and $(5(1-s)+s)\,f_s$ (for the case where $\eta = 0$). Consequently, we find bad values for global modulation indexes $m_{tsh_{(2k+1)}}$.

From this analysis, we can conclude that the monitoring of these terms (K_{pn}, m_{tc}, $m_{tsh_{(5)}}$ and $m_{tsh_{(7)}}$) allow to know if the induction motor operate with a faulty cage. Consequently, for the broken rotor bar diagnosis, we can establish a criterion which take into account this information like in [5].

B. Detection of a load torque oscillation

The load torque variation can have an unspecified frequency. The torque ripple can be synchronous or asynchronous with the position of the shaft. In practice, synchronous torque oscillation is typical for such mechanical abnormalities as rotor imbalance and eccentricity and, in an extreme case, a rub between the rotor and the stator. Consequently, the frequency of the load torque oscillation can be equal to $(1-g)f_s$ if a resistance appears, for example, at each rotation of the induction motor. If the synchronous speed of the induction motor is equal to 3000 rpm, this frequency will be approximatively equal to 46 Hz and if the synchronous speed of the motor is equal to 1500 rpm, this frequency will be equal to 23 Hz. Asynchronous torque oscillation, on the other hand, may result from abnormalities in a load that is geared to the motor, or from torsional vibration of the rotor shaft. In this paper, we study the case of a load torque frequency equal to $2sf_s$ because it induces, in the line current spectrum (frequency band [0 - 100] Hz), the same components that a broken rotor bar (figure 4(c)).

To introduce a load torque oscillation, we switch the second resistor bank on and off with a frequency of 6.5 Hz. This frequency corresponds to a frequency of $2sf_s$ when the motor operate with its nominal torque (we chose a oscillation frequency equal to the $2sf_s$ frequency detected in the case of a healthy rotor for each load level studied). The value of the second resistor bank was chosen to have an amplitude of the component at $(1+2s)f_s$ in the line current spectrum identical to that obtained in the case of a broken rotor bar (see figures 4(b) and 4(c)).

In this configuration, we find, in the low frequency band of the instantaneous power, components at frequencies $2ksf_s$ as we can see on figure 3(c). In this case, the amplitude of the component at $2sf_s$ is largest, which makes it possible to use the same method developed in section II for the calculation of the slip of the induction motor. With this value, we calculate frequencies $(1 \pm 2ks)f_s$ and $(x(1-s) \pm (1+2\eta)s)\,f_s$ to evaluate global modulation indexes m_{tc} and $m_{tsh_{(2x+1)}}$.

Results in this configuration are referred in Table I (lines noted LTV: Load Torque Variation). As we can see, the global modulation index m_{tc} and the number of components K_{pn} increase when a load torque oscillation is introduce by the second resistor bank. However, we can see that global modulation indexes of space harmonics are not disrupted by this fault. Indeed, the augmentation of these indexes is much lower than in the case of a fault cage (figure 5(c)). This result show us that the study of space harmonics is essential to differentiate a broken rotor bar to a load torque oscillation at $2sf_s$.

VI. Conclusion

The instantaneous power spectrum gives additional components to the modulation frequency $2ksf_s$. These are the result of the disturbance to the induction motor. The diagnosis based on the global modulation index method applied to the line current signal provides relevant results for the detection of broken rotor bars and load torque oscillation. We have demonstrated that the study of components created by space harmonics allow to differentiate a broken bar to a load torque oscillation when the latter has a frequency equal to $2sf_s$. The experimental results show the effectiveness of the technique, even if the motor operates under a low load. The monitoring of the global modulation index m_{tc} enabled us to detect a partially broken bar in the rotor cage. Moreover, we showed that the measurement of the instantaneous power of a stator phase can be used to calculate the slip of the asynchronous machine. The frequencies of the characteristic components (load torque variation or broken rotor bar) are clear from the supply frequency, which enables the detection to be easily highlighted.

References

[1] W.T. Thomson and M. Fenger, "Current Signature Analysis to Detect Induction Motor Faults," *IEEE Transactions on IAS Magazine*, Vol. 7, No. 4, pp. 26-34, July/August 2001.

[2] F. Filipetti and G. Franceschini and C. Tassoni and P. Vas, "Impact of speed ripple on rotor fault diagnosis of induction machine," *International Conference on Electrical Machines*, Vol. 2, Vigo, Spain, pp. 452-457, September 10-12, 1996.

[3] W. Deleroi, "Broken Bar in Squirrel-Cage Rotor of an Induction Motor. Part I: Description by Superimposed Fault-Currents," *Archiv Fur Elektrotechnik*, Vol. 67, pp. 91-99, 1984.

[4] G. Didier and H. Razik and A. Rezzoug, "On the Modelling of Induction Motor Including the First Space Harmonics for Diagnosis Purposes," *International Conference on Electrical Machines*, August 2002.

[5] G. Didier and H. Razik and O. Caspary and E. Ternisien, "Rotor Cage Fault Detection in Induction Motor using Global Modulation Index on the Instantaneous Power Spectrum," *SDEMPED'03* , August 2003.

[6] R. Maier, "Protection of Squirrel Cage Induction Motor Utilizing Instantaneous Power and Phase Information," *IEEE Transactions on Industry Applications*, Vol. 28, No 2, pp. 376-380, March/April 1992.

[7] S.F. Legowski and A.H.M. Sadrul Ula and A.M. Trzynadlowski, "Instantaneous Power as a medium for the Signature Analysis of Induction Motors," *IEEE Transactions on Industry Electronics*, Vol. 47, No 5, pp. 984-993, October 2000.

[8] A.M. Trzynadlowski and S.F. Legowski, "Diagnosis of Mechanical Abnormalities in Induction Motors Using Instantaneous Electric Power," *IEEE Transactions on Energy Conversion*, Vol. 14, No 4, pp. 1417-1423, December 1999.

[9] A.M. Trzynadlowski and E. Ritchie, "Comparative Investigation of Diagnosis Media for Induction Motor: A Case of Rotor Cage Faults," *IEEE Transactions on Industry Electronics*, Vol. 47, No 5, pp. 1092-1099, October 2000.

[10] M.S. Bartlett, "Smoothing Periodograms from Time Series with Continuous Spectra," *Nature*, London, vol. 161, pp. 686-687, May 1948.

[11] S.L. Marple, "Digital Spectral Analysis with Applications," *Prentice-Hall*, New Jersey, 1987.

TABLE I

GLOBAL MODULATION INDEX m_{tc} OF THE LINE CURRENT.

State of the motor	Frequency $2sf_s$	Speed	K_{pn}	m_{t_c}	$\mathcal{A}(m_{tc})$	m_{tsh_5}	$\mathcal{A}(m_{tsh_5})$	m_{tsh_7}	$\mathcal{A}(m_{tsh_7})$
H-L100	6,53	2803	2	0,0021		0,0014		0,0011	
05b-L100	5,98	2820	3	0,0053	+153%	0,0032	+128%	0,0016	+45%
1b-L100	6,67	2799	3	0,0408	+1843%	0,0236	+1585%	0,0102	+827%
LTV-L100	6,41	2807	5	0,0239	+1038%	0,0017	+21%	0,0013	+23%
H-L75	4,94	2851	3	0,0024		0,0013		0,0011	
05b-L75	4,27	2872	3	0,0070	+192%	0,0041	+215%	0,0021	+91%
1b-L75	4,64	2860	4	0,0442	+1742%	0,0314	+2315%	0,0138	+1154%
LTV-L75	4,94	2851	5	0,0277	+1054%	0,0021	+61%	0,0015	+36%
H-L50	3,17	2904	2	0,0018		0,0015		0,0015	
05b-L50	2,87	2913	3	0,0038	+111%	0,0039	+160%	0,0017	+13%
1b-L50	2,99	2910	4	0,0350	+1844%	0,0248	+1553%	0,0103	+586%
LTV-L50	3,05	2908	9	0,0380	+2011%	0,0021	+40%	0,0017	+13%
H-L25	1,59	2952	2	0,0048		0,0013		0,0016	
05b-L25	1,47	2956	2	0,0100	+108%	0,0039	+20%	0,0014	-12%
1b-L25	1,53	2954	3	0,0281	+485%	0,0204	+1470%	0,0093	+481%
LTV-L25	1,59	2952	8	0,0359	+648%	0,0028	+115%	0,0028	+75%
H-L0	0,30	2990	1	0,0046		Not detected			
05b-L0	0,27	2993	1	0,0069	+50%	Not detected			
1b-L0	0,27	2993	2	0,0065	+41%	Not detected			

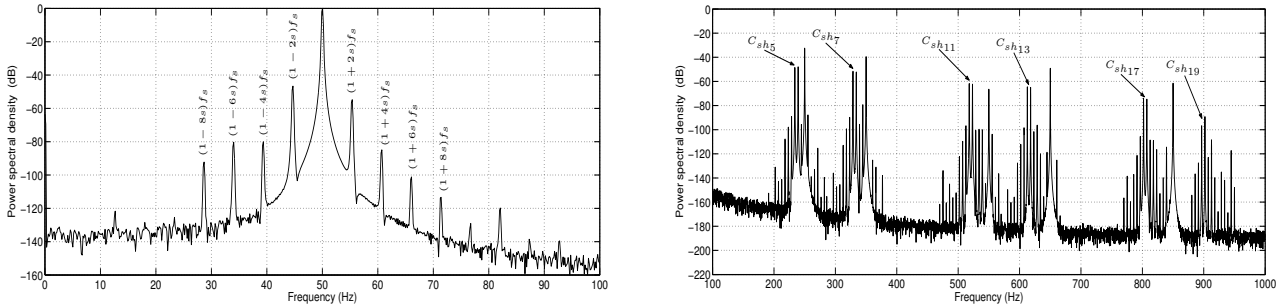

(a) (b)

Fig. 1. Line current spectrum with one broken rotor bar in the frequency band: (a) [0 - 100] Hz, (b) [100 - 1000] Hz (Simulation results).

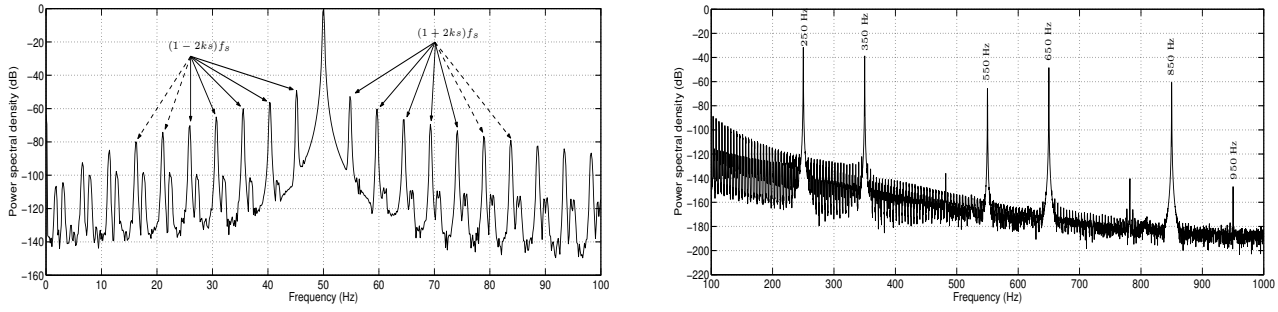

(a) (b)

Fig. 2. Line current spectrum with a load torque variation: (a) in the frequency band [0 - 100] Hz, (b) in the frequency band [100 - 1000] Hz (Simulation results).

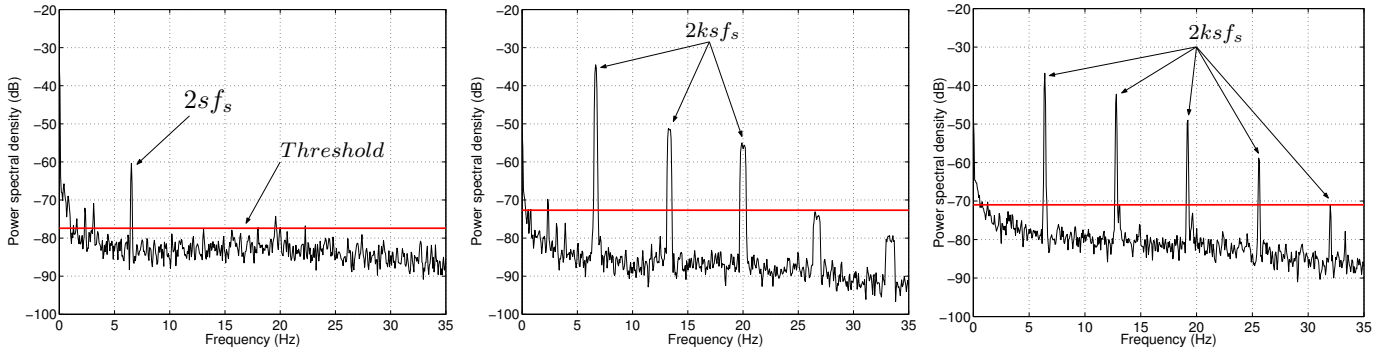

(a) Healthy rotor (b) One broken rotor bar (c) Load torque variation

Fig. 3. Instantaneous power spectrum in the frequency band [0-35] Hz (Experimental results).

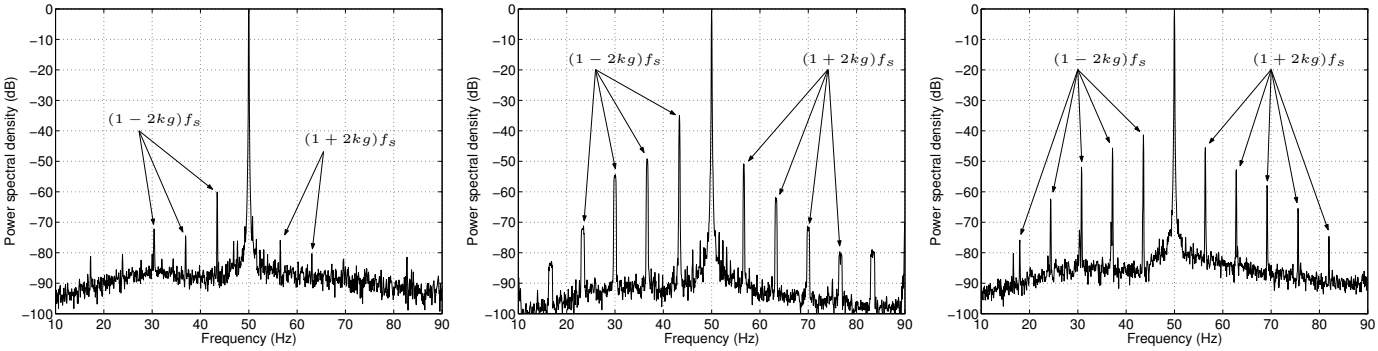

(a) Healthy rotor (b) One broken rotor bar (c) Load torque variation

Fig. 4. Line current spectrum in the frequency band [10-90] Hz (Experimental results).

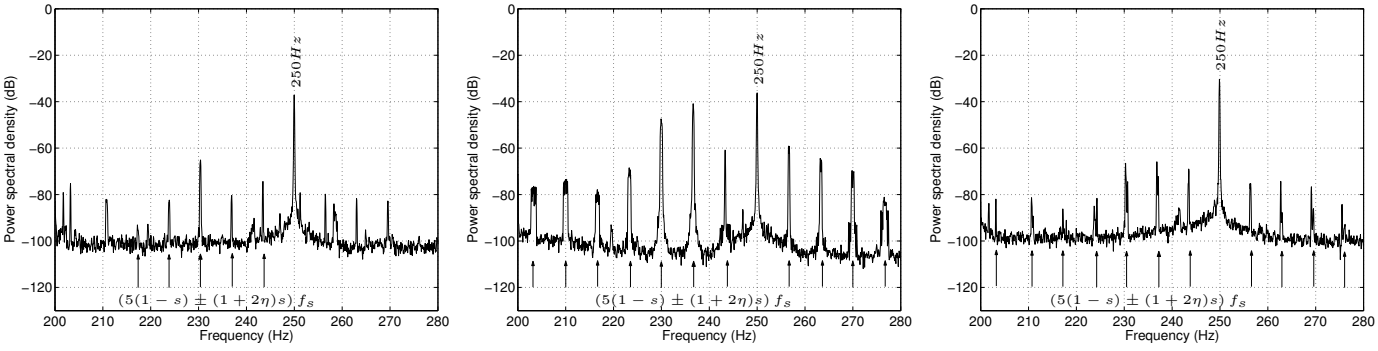

(a) Healthy rotor (b) One broken rotor bar (c) Load torque variation

Fig. 5. Line current spectrum in the frequency band [200-280] Hz (Space harmonic 5) (Experimental results).